Arabian Journal of Chemistry (2017) **10**, 253–261

King Saud University

Arabian Journal of Chemistry

www.ksu.edu.sa
www.sciencedirect.com

ORIGINAL ARTICLE

Green biosynthesis of silver nanoparticles using *Calliandra haematocephala* leaf extract, their antibacterial activity and hydrogen peroxide sensing capability

Selvaraj Raja *, **Vinayagam Ramesh, Varadavenkatesan Thivaharan**

Department of Biotechnology, Manipal Institute of Technology, Manipal, Karnataka 576104, India

Received 9 April 2015; accepted 16 June 2015
Available online 27 June 2015

KEYWORDS

Calliandra haematocephala;
Green synthesis;
Silver nanoparticles;
Hydrogen peroxide;
Zeta potential;
Gallic acid

Abstract In recent times, plant-mediated synthesis of nanoparticles has garnered wide interest owing to its inherent features such as rapidity, simplicity, eco-friendliness and cheaper costs. For the first time, silver nanoparticles were successfully synthesized using *Calliandra haematocephala* leaf extract in the current investigation. The as-formed silver nanoparticles were characterized by UV–Vis spectrophotometer and the characteristic surface plasmon resonance peak was identified to be 414 nm. The morphology of the silver nanoparticles was characterized by scanning electron microscopy (SEM) and energy dispersive spectroscopy (EDS) was used to detect the presence of elemental silver. X-ray diffraction (XRD) was employed to ascertain the crystalline nature and purity of the silver nanoparticles which implied the presence of (1 1 1) and (2 2 0) lattice planes of the face centered cubic (fcc) structure of metallic silver. Fourier transform infrared spectroscopy (FTIR) was used to key out the specific functional groups responsible for the reduction of silver nitrate to form silver nanoparticles and the capping agents present in the leaf extract. The stability of the silver nanoparticles was analyzed by zeta potential measurements. A negative zeta potential value of −17.2 mV proved the stability of the silver nanoparticles. The antibacterial activity against *Escherichia coli* – pathogenic bacteria – and the capacity to detect hydrogen peroxide by the silver nanoparticles were demonstrated which would find applications in the development of new antibacterial drugs and new biosensors to detect the presence of hydrogen peroxide in various samples respectively.

* Corresponding author. Tel.: +91 820 2924322; fax: +91 820 2571071.
E-mail address: rajaselvaraj@gmail.com (S. Raja).
Peer review under responsibility of King Saud University.

Production and hosting by Elsevier

http://dx.doi.org/10.1016/j.arabjc.2015.06.023

1. Introduction

Versatile applications of silver nanoparticles such as antimicrobial effect (Khan et al., 2014; Kumar et al., 2014), antitumor effect (Jeyaraj et al., 2013), sensitivity to detect the presence of various pollutants such as metals (Balavigneswaran et al., 2014), dyes (Kumar et al., 2013), antibiotics (Singh et al., 2012) and nitro-aromatic compounds (Narayanan and Sakthivel, 2011) in industrial effluents attracted many scientists to pursue research in nanobiotechnology. It has been shown by many researchers that the conventional methods of synthesis of silver nanoparticles have many limitations. Such processes are usually slow, have a high cost and involve use of chemical reducing agents such as sodium borohydride, trisodium citrate and dimethyl formamide, which pose an environmental burden. In most of the cases, the silver nanoparticles formed are highly unstable and necessitate the addition of a separate capping agent which renders stability.

In contrast, the green synthesis of silver nanoparticles gained a lot of attention owing to the instinctive features such as usage of natural resources, rapidness, eco-friendliness and benignancy. These appealing features are essential in medical applications. The other advantages of green synthesis include well-defined and controlled size of the nanoparticles. They are devoid of contaminants and the process is easy to scale-up (Mittal et al., 2013).

One of the green methods of synthesis of nanoparticles is the utilization of various plants and their parts. The various biomolecules present in the plant extract such as enzymes, proteins, flavonoids, terpenoids and cofactors act as both reducing and capping agents (Tavakoli et al., 2015). The plant-mediated synthesis of nanoparticles is relatively fast as there is no need of maintaining specific media and culture conditions, unlike microbial synthesis.

Recent literature reveals the use of leaf extract from various plants such as *Azadirachta indica* (Nazeruddin et al., 2014), *Delonix elata* (Sathiya and Akilandeswari, 2014), *Tephrosia purpurea* (Ajitha et al., 2014), *Melia dubia* (Kathiravan et al., 2014), *Tribulus terrestris* (Ashokkumar et al., 2014), *Artemisia nilagirica* (Vijayakumar et al., 2013), *Boerhaavia diffusa* (Kumar et al., 2014), *Ficus religiosa* (Antony et al., 2013), *Piper pedicellatum* C.DC (Tamuly et al., 2013) and *Melia azedarach* L. (Mehmood et al., in press), as sources for synthesis of silver nanoparticles.

Thence, in the present study, the aqueous extract of leaves obtained from *Calliandra haematocephala* was studied for the synthesis of silver nanoparticles. *C. haematocephala*, a shrub, commonly known as red powder puff, is a flowering ornamental plant, belonging to the genus *Calliandra* in the *Fabaceae* family. It is a traditional medicinal plant that grows to a height of 2–5 m and is 2–3 m wide. The leaves of this plant contain large amounts of imino acids that offer fungal resistance (Brenner and Romeo, 1986).

Various imino acids such as pipecolic acid, *trans*-4 and *trans*-5-hydroxypipecolic acid, *trans–cis*-4,5-dihydroxypipecolic acid and *trans*-4-acetylaminopipecolic acid are reported to be present in the leaves of *C. haematocephala* by Romeo (1984). The author demonstrated the insecticidal activity of imino acids present in the leaves against *Spodoptera frugiperda*. The antisickling property of the leaf and root extracts was validated by Amujoyegbe et al. (2014).

The antibacterial activity of bark extract of *C. haematocephala* was studied by Nia et al. (1999). The gastroprotective activity of *C. haematocephala* extracts was evaluated by de Paula Barbosa et al. (2012). The use of this plant in traditional medicine can be attributed to the presence of tannins, flavonoids and saponins, as suggested by the phytochemical investigations.

Moharram et al., 2006 reported the various phytochemicals present in the stem and leaves of *C. haematocephala* and identified their structure. Few of the compounds include gallic acid, methyl gallate, caffeic acid, myricitrin, quercitrin, afzelin and isoquercitrin. The presence of these compounds imparts radical scavenging property to this plant. The authors also demonstrated the lethal effect of myricitrin and quercitrin toward the shrimp *Artemia salina*.

Hydrogen peroxide (H_2O_2) is a strong oxidizing agent which is widely used in food, pharmaceutical, cosmetics, wood and pulp industries. However, the exposure and the presence of even a small of amount of H_2O_2 in process streams result in various health and environmental hazards due to its toxicity (Tagad et al., 2013). Therefore it is essential to develop accurate and fast methods to detect H_2O_2.

Bera and Raj, 2013 used triangular silver nanoplates for the detection of H_2O_2. Liu et al., 2013 developed a H_2O_2 sensor based on silver nanoparticles biosynthesized by *B. subtilis*. Wang and Yun, 2013 developed a non-enzymatic sensor for H_2O_2 based on the electrodeposition of silver nanoparticles on poly (ionic liquid)-stabilized graphene sheets and they demonstrated the detection of H_2O_2 in commercially available products such as honey and milk. Recently, Mohan et al., 2014 exploited the silver nanoparticles synthesized from dextrose for the optical sensing of H_2O_2. A cost-effective, reliable and more specific method for the detection of H_2O_2 is sought in the present investigation.

Literature reveals that there are no reports available for the synthesis of nanoparticles using the aqueous extract of *C. haematocephala* leaves. Therefore, the objective of the present study was to synthesize and characterize the silver nanoparticles using the leaf extract of *C. haematocephala*. In addition, the antibacterial activity and the ability to detect H_2O_2 were also investigated.

2. Materials and methods

2.1. Chemicals

Silver nitrate and hydrogen peroxide were procured from Merck, India. The nutrient agar and other media components were purchased from Sisco Research Laboratories (SRL), Mumbai, India. The glassware used in the current study was acid-washed thoroughly and then rinsed with Millipore-Milli-Q water.

2.2. Collection, processing and preparation of *C. haematocephala* leaf extract

Fresh leaves of *C. haematocephala* were collected in the month of March, in Manipal University precincts, Manipal. The plant was taxonomically identified and authenticated by Ms. Usharani S. Suvarna, Head of the Department of Botany, MGM College, Udupi, India. The leaves were thoroughly

washed under tap water to remove the adhered dust particles present on the surface and then rinsed with Millipore-Milli-Q water. The cleaned leaves were completely dried at room temperature on a blotting paper. The dried leaves were chopped into small pieces and stored in an air-tight container at room temperature for further use. The aqueous leaf extract of *C. haematocephala* was prepared as follows: 10 g of chopped leaves were mixed with 100 mL of water in a 250 mL flask and the contents were boiled for 10 min. The contents were cooled to room temperature and filtered through Whatman No. 1 filter paper. The clear leaf extract of *C. haematocephala* thus obtained was used for synthesis of silver nanoparticles.

2.3. Synthesis of silver nanoparticles

In order to synthesize silver nanoparticles (SNPs), 10 mL of the leaf extract was mixed with 90 mL of 1 mM silver nitrate solution and heated in a water bath, set at 80 °C for 10 min. A color change from yellow to brown designates the formation of colloidal SNPs.

2.4. Characterization of silver nanoparticles

The formation of silver nanoparticles was monitored periodically by UV–Vis spectra in a wavelength range of 200–800 nm at a resolution of 1 nm using Shimadzu spectrophotometer (Model UV 1700). The samples were appropriately diluted with water before each measurement. In order to remove the unbound moieties from the SNPs, the supernatant formed after centrifugation at 22,360*g* for 15 min was disposed. The pellet was then dispersed with distilled water. The procedure was repeated thrice. The purified pellets were dried in a hot air oven at 80 °C for 12 h and the dried SNPs were scrapped out for further characterization using FTIR spectroscopy. The FTIR spectrum was obtained with Shimadzu8400S spectrophotometer using potassium bromide pellets at a resolution of 4 cm^{-1} in the diffuse reflectance mode.

X-ray diffraction analysis was performed to examine the crystallographic structure of the purified SNPs. In the procedure for preparing samples for XRD, a thin film of sample was applied onto a glass slide by dropping 100 μL of the sample and drying for 30 min. The XRD pattern was recorded using Rigaku Miniflex 600 X-ray diffractometer with operating voltage of 40 kV at a 15 mA current strength. The samples were subjected to Cu Kα radiation with nickel monochromator in the 2θ range of 20–80°.

The same sample preparation procedure was used for scanning electron microscope (SEM) and energy dispersive spectrum (EDS) measurements. A scanning electron microscope (EVO MA18) coupled with energy dispersive X-ray (EDX) analysis (Oxford) was used for the analysis.

Dynamic light scattering method was employed for the zeta potential and particle size analysis of the colloidal SNPs using Malvern Zetasizer nanosizer (size range 0.1–10,000 nm).

2.5. Antibacterial activity

The silver nanoparticles synthesized using the *C. haematocephala* leaf extract were tested for the antimicrobial activity by standard agar-well diffusion method. *Escherichia coli*, human pathogenic bacteria was used as the test specimen. A pure culture of *E. coli* was sub-cultured in nutrient broth and the strain was uniformly spread on sterilized petri plates. Two circular wells, A and B, of 6 mm diameter were made using a sterile cork-borer. The well B was loaded with a chemical antibiotic, chloramphenicol (50 μL) as a positive control and the well A was loaded with 50 μL silver nanoparticles to check the antibacterial activity. The plates were incubated at 37 °C overnight and the zones of inhibition were observed.

2.6. Hydrogen peroxide-sensing capacity of silver nanoparticles

With the objective of verifying the sensing capacity of silver nanoparticles to detect H_2O_2, the protocol developed by the researchers Bera and Raj, 2013 was used. The initial spectrum of appropriately diluted SNP solution (3 mL) was noted using the spectrophotometer. 1 mL of 20 mM H_2O_2 was added to the SNP solution and thoroughly mixed. The spectrum readings were taken at regular intervals and the change in spectra was noted.

3. Results and discussion

3.1. UV–Vis spectra analysis

The reduction of silver nitrate to silver nanoparticles by the leaf extract of *C. haematocephala* was confirmed by measuring the UV–Vis spectrum of the colloidal solution. The silver nitrate solution (B) was added to the yellow aqueous leaf extract (C) and heated for 10 min at 80 °C. The color change to brown (D) confirmed the formation of silver nanoparticles (Fig. 1).

This color change was due to the reduction of Ag^+ to Ag^0 by various biomolecules present in the leaf extract. The absorption spectra of silver nitrate, leaf extract and the silver nanoparticles were recorded and are depicted in Fig. 2. Both silver nitrate and the leaf extract did not have a peak in the visible range. In contrast to this, the SNPs showed a characteristic absorption peak at a wavelength of 414 nm because of surface plasmon resonance (SPR). This SPR peak is very sensitive to the size and shape of the nanoparticles, amount of extract, silver nitrate concentration and the type of biomolecules present in the leaf extract. The spherical shape of the as-synthesized silver nanoparticles was confirmed by the λ_{max} of 414 nm. According to the literature (Prathna et al., 2011), absorption bands in the range 400–420 nm in the UV-Vis spectrum correspond to spherical-shaped metallic nanoparticles. The presence of a single peak in the figure corroborated the spherical shape of the as-formed SNPs according to Mie theory (Prathna et al., 2011).

Similar kind of results were observed by Rastogi and Arunachalam (2011) for the SNPs synthesized using the aqueous garlic extract (λ_{max} = 414) under sunlight irradiation and by Suman et al., 2013 for the SNPs synthesized using the root extract of *Morinda citrifolia* (λ_{max} = 413 nm).

The stability of the nanoparticles as a function of time was monitored using the spectrophotometer. The absorption band (λ_{max}) was constant for more than 30 days which substantiated the stability of the nanoparticles (data not shown).

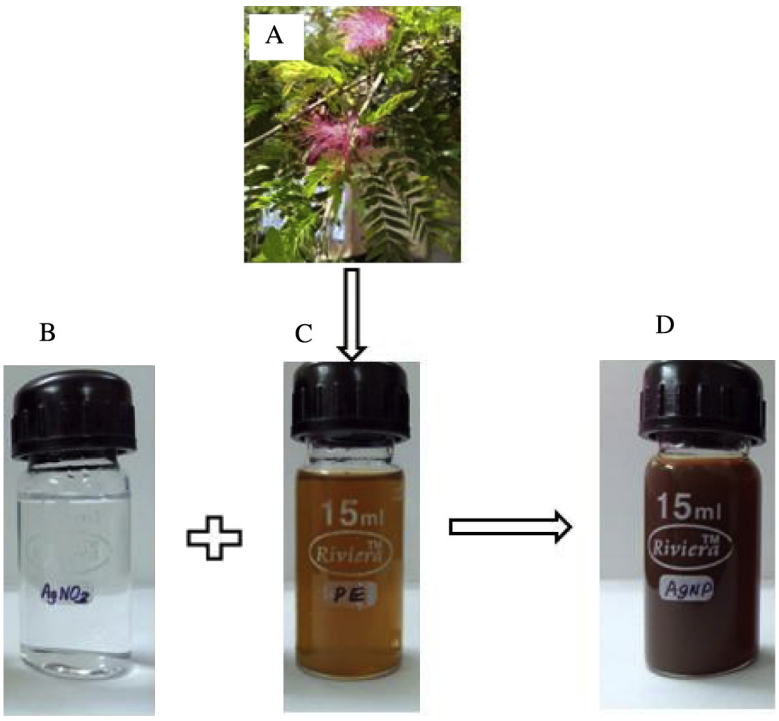

Figure 1 Formation of SNPs (A = *Calliandra haematocephala* plant, B = Silver nitrate solution, C = Leaf extract, D = Silver nanoparticles).

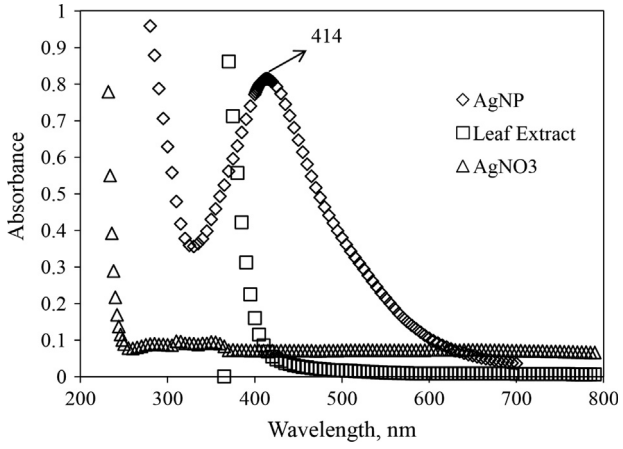

Figure 2 UV–Vis spectra of SNPs synthesized using the leaf extract of *Calliandra haematocephala*.

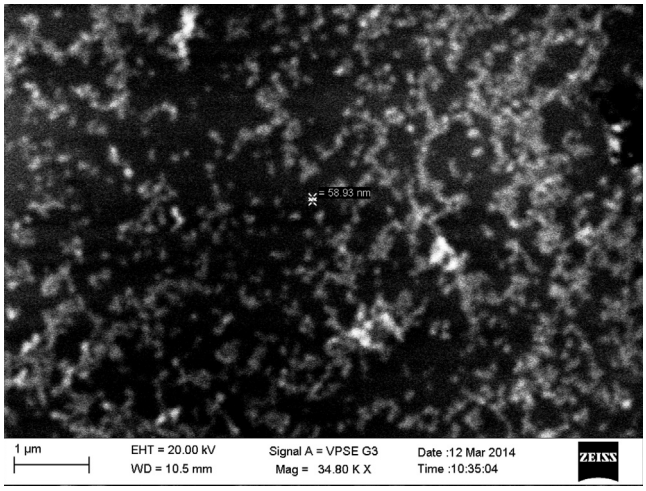

Figure 3 SEM image with 34,800× magnification of SNPs synthesized using the leaf extract of *Calliandra haematocephala*.

3.2. SEM with EDS analysis

The surface morphology and topography of the SNPs were examined by scanning electron microscopy (Fig. 3). Well-defined spherical SNPs without any agglomeration were evidenced from the figures. The average particle size within the selected area of SEM image was 70 nm, conforming to the nano-range. The result is comparable with the *A. nilagirica* leaf extract-mediated silver nanoparticles by Vijayakumar et al. (2013).

Energy dispersive spectrum revealed the presence of elemental silver in the sample (Fig. 4). The sharp peak at 3 keV denoted the existence of metallic silver. The occurrence of other peaks (Ca, Si and Na) was presumably related with the glass underneath, which held the sample (Zhang et al., 2011).

3.3. X-ray diffraction

The X-ray diffraction (XRD) profile of SNPs synthesized using the leaf extract of *C. haematocephala* is depicted in Fig. 5. The two distinct peaks at $2\theta = 38.78°$ and $65.14°$ were understood to be (1 1 1) and (2 2 0) lattice planes respectively, to the face-centered cubic (fcc) structure of metallic silver. This is in accordance with the standard metallic silver XRD pattern JCPDS No. 04-0873. The intense diffraction peak of (1 1 1)

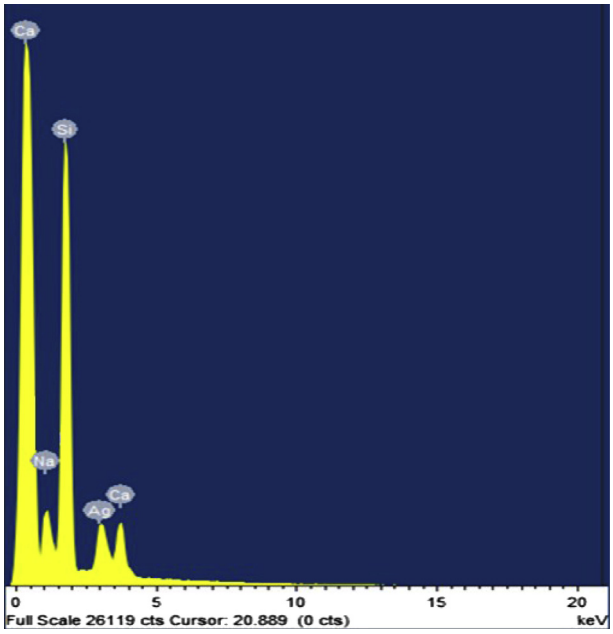

Figure 4 EDS of SNPs synthesized using the leaf extract of *Calliandra haematocephala*.

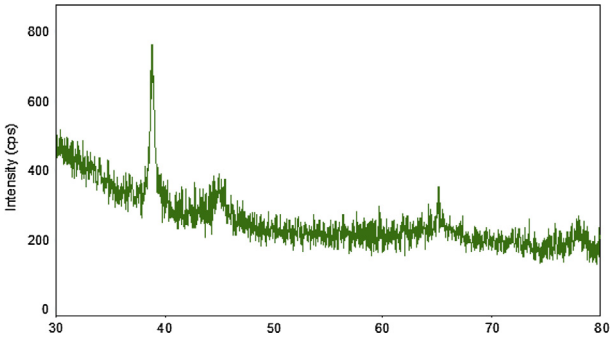

Figure 5 XRD pattern of SNPs synthesized using the leaf extract of *Calliandra haematocephala*.

substantiated that the synthesized SNPs might be enriched with (1 1 1) facets [10]. Non-appearance of other peaks confirmed the purity of SNPs used in the analysis. The size of the SNPs was calculated by Debye–Scherrer equation (Cullity, 1978) as follows:

$$S = k\lambda/\beta_{0.5}\cos\theta$$

where S is the crystallite size of SNPs, λ is the wavelength of the X-ray source (1.54056 Å) used in XRD, $\beta_{0.5}$ is the full width at half maximum (FWHM) of the diffraction peak in radian, k is the Scherrer constant that varies from 0.9 to 1 and θ is the Bragg angle in radian.

The various calculation parameters including the lattice parameter and crystal sizes are shown in Table 1. In the present XRD pattern, the average size of nanoparticles was calculated as 13.07 nm. The lattice parameters were 0.4018 nm and 0.4047 nm for (1 1 1) and (2 2 0) planes respectively. The calculated values are concordant with the standard lattice parameter of 0.40729 nm for metallic silver (Theivasanthi and Alagar, 2012).

3.4. Particle size analysis

Dynamic light scattering (DLS) measurements were done to determine the size of the SNPs formed. The particle size distribution curve of the synthesized SNPs is shown in Fig. 6. It showed various sizes of the particles ranging from 13.54 nm to 91.28 nm and had an average particle size of 104.3 nm. Precisely, 24.5% of total particles had the size of 15.69 nm, 18.17% had 28.9 nm and 21.04% had 18.9 nm. Moreover, the difference between the largest and the smallest size of the nanoparticles was 73.96 nm which indicated the narrow distribution of the SNPs (Ghorbani, 2013).

In addition to this, the zeta potential value was determined as −17.2 mV (Fig. 7), a measure of stability of the nanoparticles. The negative value indicated the stability of the nanoparticles and it evaded the agglomeration of nanoparticles (Patil et al., 2012). The result is consistent with the silver nanoparticles synthesized from the leaf extract of *F. religiosa* (Antony et al., 2013). The negative potential value might be due to the capping action of biomolecules present in the leaf extract of *C. haematocephala*.

3.5. FT-IR spectroscopy

With the objective of finding various functional groups responsible for the reduction of silver nitrate to silver nanoparticles, FTIR studies were carried out. As shown in Fig. 8, the FTIR spectrum exhibited a number of major peaks positioned

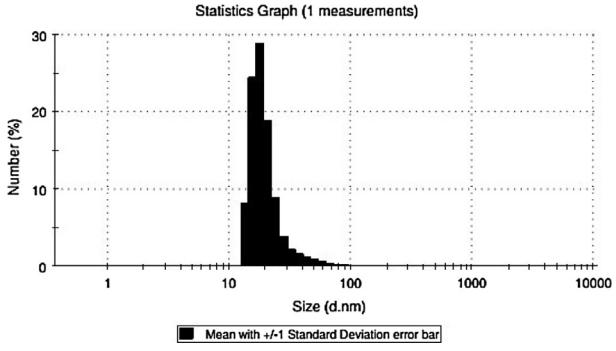

Figure 6 Particle size distribution curve for SNPs synthesized using the leaf extract of *Calliandra haematocephala*.

Table 1 Characteristic XRD parameters of bio-synthesized SNPs from the leaf extract of *Calliandra haematocephala*.

2θ (degree)	Plane (hkl)	Interplanar spacing (nm)	Lattice parameter (nm)	FWHM (rad)	Crystallite size (nm)
38.78	(1 1 1)	0.232	0.4018	0.0083	19.69
65.14	(2 2 0)	0.143	0.4047	0.0283	6.45

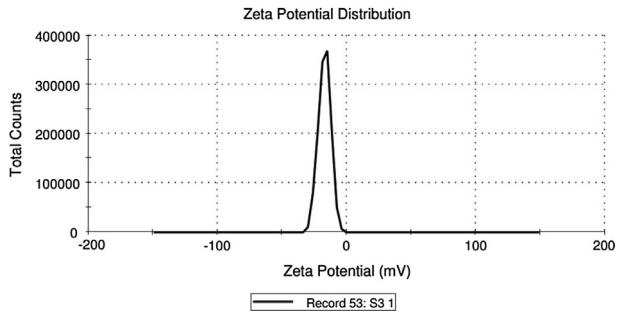

Figure 7 Zeta potential for SNPs synthesized using the leaf extract of *Calliandra haematocephala*.

at 3548.78, 3487.06, 3379.05, 2931.60, 2352.99, 1720.39, 1620.09, 1442.66, 1380.94, 1218.93, 1049.20, 825.48 and 663.47 cm^{-1}. The existence of peaks at 3548.78, 3487.06 and 3379.05 might be due to the —OH stretching of alcohols and phenols or bending stretching of hydrogen-bonded alcohols and phenols in the leaf extract. Shanmugam et al., 2014 suggested that these bonds could be due to the stretching of —OH in proteins, enzymes or polysaccharides present in the extract. The small band at 2931.60 was due to the —CH stretching of alkanes. The analogous scissoring and bending vibration was observed at 1442.66 and 1380.94. The medium band observed at 1720.39 implied the stretching vibrations of C═O functional groups of aldehydes, ketones and carboxylic acids.

A strong peak at 1620.09 denoted the bending vibrations of amide I group and suggested the possible binding of SNPs with the proteins present in the extract. This is in agreement with SNP from leaf extract of *Mimusops elengi* Linn (Prakash et al., 2013). The small peaks at 1218.93 and 1049.20 connoted the C—O stretching of esters or C—N stretching vibrations of amines present in the extract. The band observed at 663.47 might be because of the α-glucopyranose rings deformation of carbohydrates (Yang et al., 2009). Ajitha et al., 2014 suggested that it might be due to the C—Cl stretching modes of alkyl halides present in the extract. The peak obtained at 825.48 witnessed the bending vibrations of C—H groups of phenyl rings.

The unique strong absorption band observed at 2352.99 might be referred to thiol group (—SH) vibration of L-cysteine amino acid (Wang et al., 2009). The presence of this peak affirmed the fact that the SNPs were capped by L-cysteine present in the leaf extract. The phenomenon of capping action by L-cysteine and the stability was explained by Perni et al. (2014) for the SNP synthesis using *E. coli*. This is further supported by the finding of Mishra and Sardar, 2012, who concluded that the free thiol groups present in the proteins were responsible for the reduction of silver nitrate to silver nanoparticle formation. Therefore, from the above FTIR spectra details, it was evident that the presence of various biomolecules in the leaf extract played a major role in the reduction and stability of SNPs.

As mentioned earlier, the leaf extract of *C. haematocephala* contains gallic acid. This could be responsible for the reduction

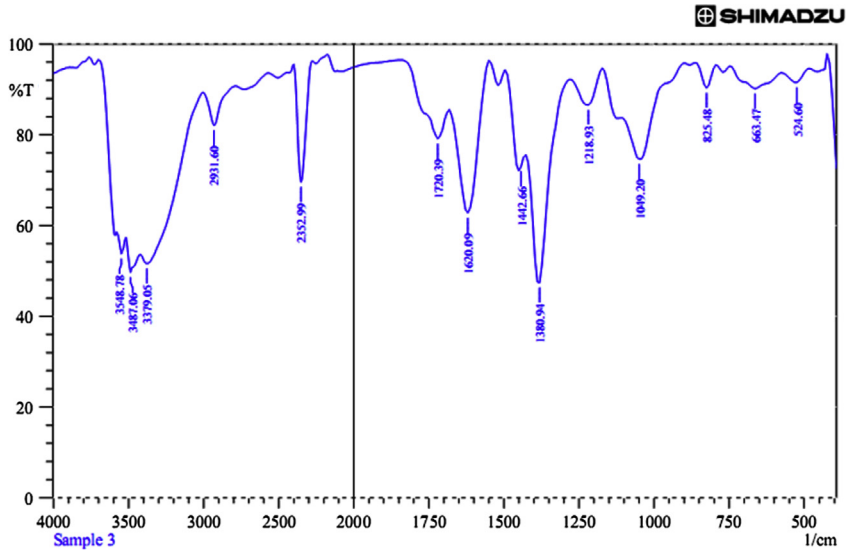

Figure 8 FT-IR spectra of SNPs synthesized using the leaf extract of *Calliandra haematocephala*.

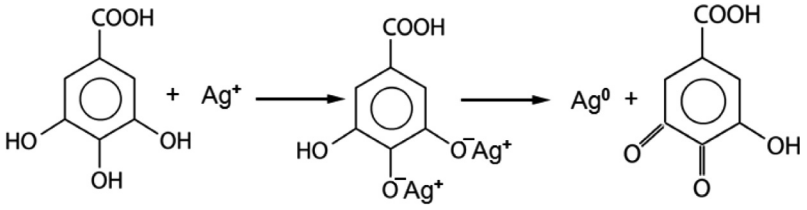

Figure 9 Mechanism of SNP (Ag^0) formation from gallic acid present in the leaf extract of *Calliandra haematocephala*.

of silver nitrate to silver nanoparticles and provision of stability. According to Wang et al., 2007, gallic acid is known to reduce metallic salt to form nanoparticles. As reported by Edison and Sethuraman (2012), Ag^+ ions form intermediate complexes with phenolic groups present in gallic acid. These complexes consequently reduce Ag^+ to SNPs with concomitant oxidation to quinone form. The plausible mechanism is shown in Fig. 9. A similar result was obtained by Martínez-Castañón et al. (2008) using gallic acid to synthesize SNPs with various sizes.

3.6. Antibacterial activity

The renowned inhibitory effect of silver has been known for many years and used for various medical applications (Geethalakshmi and Sarada, 2012). In order to examine the antibacterial activity of the silver nanoparticles synthesized using *C. haematocephala* leaf extract, well diffusion method was employed (Fig. 10). 50 µL of silver nanoparticles was loaded into the well A and 50 µL chloramphenicol (as a positive control) was loaded into the well B. The inhibition zone observed around the well A encompassed the antibacterial potential of SNPs; this was comparable to that around well B.

There are various mechanisms proposed in the literature for the antimicrobial effect of SNPs. Patil et al., 2012 claimed that the cell death arising out of exposure to SNPs might be due to the cytoplasmic membrane disorganization and the consequent leakage of various biomolecules such as amino acids, protein and carbohydrates. Moreover, they indicated that the cell death could be because of inhibition of various essential enzymes. The change in membrane permeability caused by the action of silver nanoparticles as a function of conductivity was studied by Krishnaraj et al. (2010). Their study concluded that the high conductivity of cells treated with SNPs was due to the release of cellular components present inside the cells.

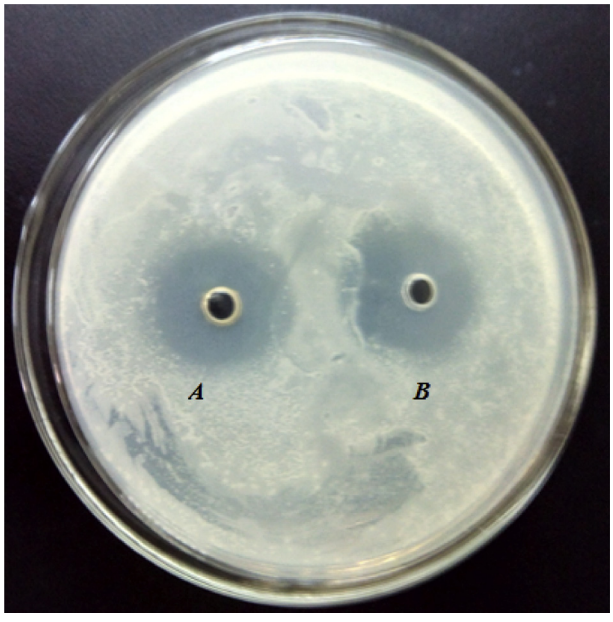

Figure 10 Antibacterial activity of silver nanoparticles synthesized using the leaf extract of *Calliandra haematocephala* against *E. coli*.

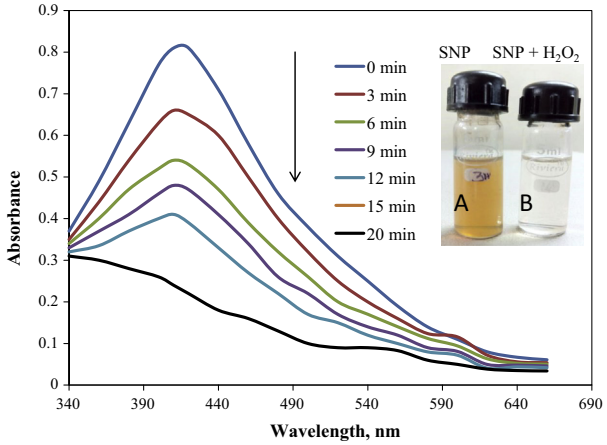

Figure 11 Effect of SNPs synthesized using the leaf extract of *Calliandra haematocephala* on 20 mM H_2O_2 solution as a function of time.

Tamboli and Lee, 2013 demonstrated that the antimicrobial effect of SNPs was due to the breakage of double-stranded DNA molecules present in the bacteria. The pronounced antibacterial effect in the present study may provide a new platform in the field of development of new antibacterial drugs.

3.7. Hydrogen peroxide-sensing capacity of SNPs

The ability of SNPs to detect the presence of H_2O_2 in a sample was affirmed by adding 1 mL of 20 mM H_2O_2 to 3 mL of appropriately diluted SNPs. The spectrum was recorded as a function of time at regular intervals. As shown in Fig. 11, a decreasing trend in absorbance was observed as the time increased and eventually the characteristic silver SPR peak at 414 nm disappeared. It was apparent from the inset in Fig. 11 that the color intensity of the SNPs (vial A) faded and finally became colorless (vial B) after 20 min. This corroborated the ability of SNPs to decompose H_2O_2 and thus provided a means of detecting its composition. The results obtained in this study are in accordance with the literature (Tagad et al., 2013). The correlation between the concentration of H_2O_2 and decrease in absorbance of SNPs as a function of time could be used as a measure to rapidly detect the H_2O_2 in the unknown samples. According to Mohan et al., 2014, the addition of SNPs to H_2O_2 resulted in the formation of free radicals which initiated the degradation of the SNPs. Subsequently, Ag^0 was oxidized to Ag^+ and a decrease in absorbance was observed. These findings suggest that the SNPs can be successfully used to detect the concentration of H_2O_2 present in various samples.

4. Conclusions

A plant-mediated, green method of synthesizing silver nanoparticles was successfully performed by employing the leaf extract of *C. haematocephala*. It was found out that the various biomolecules present in the leaf extract were responsible for the formation and stability of the SNPs. The size, morphology, crystalline structure and the stability were

characterized by UV–Vis spectroscopy, scanning electron microscopy coupled with energy dispersive spectroscopy, X-ray diffraction and dynamic light scattering respectively. The functional groups present in the SNPs were analyzed by Fourier Transform Infrared Spectroscopy. The gallic acid present in the leaf extract may play a role of reduction of silver nitrate to form SNPs. The SNPs synthesized in the present study displayed antibacterial activity against *E. coli* which suggested that they may play a role in new drug development. The sensing capacity of the SNPs toward H_2O_2 was also demonstrated. Hence the SNPs formed by this green method can be used as a probe to detect the presence of H_2O_2 in various samples.

Acknowledgments

The authors gratefully acknowledge Department of Biotechnology, MIT, Manipal University for providing the facilities to carry out the research work. They also thank Dr. Manohara Pai M.M., (Associate Director, Innovation Centre), Dr. BHS Thimmappa (Professor and Head of Department of Chemistry, MIT) and Dr. M. Sreenivasa Reddy (Professor and Head of the Department of Pharmaceutics, MCOPS) for giving permission to characterize nanoparticles in their respective departments.

References

Ajitha, B., Reddy, Y.A.K., Reddy, P.S., 2014. Biogenic nano-scale silver particles by *Tephrosia purpurea* leaf extract and their inborn antimicrobial activity. Spectrochim. Acta Part A Mol. Biomol. Spectrosc. 121, 164–172.

Amujoyegbe, O.O., Agbedahunsi, J.M., Akanmu, M.A., 2014. Antisickling properties of two *Calliandra* species: *C. portoricensis* and *C. haematocephala* (*Fabaceae*). Eur. J. Med. Plants 4, 206–219.

Antony, J.J., Sithika, M.A.A., Joseph, T.A., Suriyakalaa, U., Sankarganesh, A., Siva, D., Kalaiselvi, S., Achiraman, S., 2013. In vivo antitumor activity of biosynthesised silver nanoparticles using *Ficus religiosa* as a nanofactory in DAL induced mice model. Colloids Surf., B Biointerfaces 108, 185–190.

Ashokkumar, S., Ravi, S., Kathiravan, V., Velmurugan, S., 2014. Synthesis, characterization and catalytic activity of silver nanoparticles using *Tribulus terrestris* leaf extract. Spectrochim. Acta Part A Mol. Biomol. Spectrosc. 121, 88–93.

Balavigneswaran, C.K., Sujin Jeba Kumar, T., Moses Packiaraj, R., Prakash, S., 2014. Rapid detection of Cr(VI) by AgNPs probe produced by *Anacardium occidentale* fresh leaf extracts. Appl. Nanosci. 4, 367–378.

Bera, R.K., Raj, C.R., 2013. A facile photochemical route for the synthesis of triangular Ag nanoplates and colorimetric sensing of H_2O_2. J. Photochem. Photobiol., A 270, 1–6.

Brenner, S.A., Romeo, J.T., 1986. Fungitoxic effects of non-protein imino acids on growth of saprophytic fungi isolated from the leaf surface of *Calliandra haematocephala*. Appl. Environ. Microbiol. 51, 690–693.

Cullity, B.D., 1978. Elements of X-ray Diffraction, second ed. Addison-Wesley, MA.

de Paula Barbosa, A., da Silva, B.P., Parente, J.P., 2012. Evaluation of the gastroprotective activity of *Calliandra haematocephala* extracts. Planta Med. 78, 448.

Edison, T.J.I., Sethuraman, M.G., 2012. Instant green synthesis of silver nanoparticles using *Terminalia chebula* fruit extract and evaluation of their catalytic activity on reduction of methylene blue. Process Biochem. 47, 1351.

Geethalakshmi, R., Sarada, D.V.L., 2012. Gold and silver nanoparticles from *Trianthema decandra*: synthesis, characterization, and antimicrobial properties. Int. J. Nanomed. 7, 5375–5384.

Ghorbani, H.R., 2013. Biosynthesis of silver nanoparticles using *Salmonella typhirium*. J. Nanostruct. Chem. 3, 29–32.

Jeyaraj, M., Sathishkumar, G., Sivanandhan, G., Mubarak Alid, D., Rajesh, M., Arun, R., Kapildev, G., Manickavasagam, M., Thajuddin, N., Premkumar, K., Ganapathi, A., 2013. Biogenic silver nanoparticles for cancer treatment: an experimental report. Colloids Surf., B Biointerfaces 106, 86–92.

Kathiravan, V., Ravi, S., Ashokkumar, S., 2014. Synthesis of silver nanoparticles from *Melia dubia* leaf extract and their invitroanticancer activity. Spectrochim. Acta Part A Mol. Biomol. Spectrosc. 130, 116–121.

Khan, M., Khan, S.T., Khan, M., Adil, S.F., Musarrat, J., Al-Khedhairy, A.A., Alkhathlan, H.Z., 2014. Antibacterial properties of silver nanoparticles synthesized using Pulicaria glutinosa plant extract as a green bioreductant. Int. J. Nanomed. 9, 3551–3565.

Krishnaraj, C., Jagan, E.G., Rajasekar, S., Selvakumar, P., Kalaichelvan, P.T., Mohan, N., 2010. Synthesis of silver nanoparticles using *Acalypha indica* leaf extracts and its antibacterial activity against water borne pathogens. Colloids Surf., B Biointerfaces 76, 50–56.

Kumar, P., Govindarajua, M., Senthamilselvi, S., Premkumar, K., 2013. Photocatalytic degradation of methyl orange dye using silver (Ag) nanoparticles synthesised from *Ulva lactuca*. Colloids Surf., B Biointerfaces 103, 658–661.

Kumar, P.P.N.V., Pammi, S.V.N., Kollu, P., Satyanarayana, K.V.V., Shameem, U., 2014. Green synthesis and characterization of silver nanoparticles using *Boerhaavia diffusa* plant extract and their antibacterial activity. Ind. Crops Prod. 52, 562–566.

Liu, R., Wei, Y., Zheng, J., Zhang, H., Sheng, Q., 2013. A hydrogen peroxide sensor based on silver nanoparticles biosynthesised by *Bacillus subtilis*. Chin. J. Chem. 31, 1519–1525.

Martínez-Castañón, G.A., Niño-Martínez, N., Martínez-Gutierrez, F., Martínez-Mendoza, J.R., Ruiz, F., 2008. Synthesis and antibacterial activity of silver nanoparticles with different sizes. J. Nanopart. Res. 10, 1343–1348.

Mehmood, A., Murtaza, G., Bhatti, T.M., Kausar, R., in press. Phyto-mediated synthesis of silver nanoparticles from *Melia azedarach* L. leaf extract: characterization and antibacterial activity. Arabian J. Chem.

Mishra, A., Sardar, M., 2012. Alpha-amylase mediated synthesis of silver nanoparticles. Sci. Adv. Mater. 4, 143–146.

Mittal, A.K., Chisti, Y., Banerjee, U.C., 2013. Synthesis of metallic nanoparticles using plant extracts. Biotechnol. Adv. 31, 346–356.

Mohan, S., Oluwafemi, O.S., George, S.C., Jayachandran, V.P., Lewu, F.B., Songca, S.P., Kalarikkal, N., Thomas, S., 2014. Completely green synthesis of dextrose reduced silver nanoparticles, its antimicrobial and sensing properties. Carbohydr. Polym. 106, 469–474.

Moharram, F.A., Marzouk, M.S.A., Ibrahim, M.T., Marby, T.J., 2006. Antioxidant galloylated flavanol glycosides from C. haematocephala. Nat. Prod. Res. 20, 927–934.

Narayanan, K.B., Sakthivel, N., 2011. Heterogeneous catalytic reduction of anthropogenic pollutant, 4-nitrophenol by silver-bionanocomposite using *Cylindrocladium floridanum*. Bioresour. Technol. 102, 10737–10740.

Nazeruddin, G.M., Prasad, N.R., Waghmare, S.R., Garadkar, K.M., Mulla, I.S., 2014. Extracellular biosynthesis of silver nanoparticle using *Azadirachta indica* leaf extract and its anti-microbial activity. J. Alloys Compd. 583, 272–277.

Nia, R., Adesanya, S.A., Okeke, I.N., Illoh, H.C., Adesina, S.J., 1999. Antibacterial constituents of *Calliandra haematocephala*. Niger. J. Nat. Prod. Med. 3, 58–60.

Patil, S.V., Borase, H.P., Patil, C.D., Salunke, B.K., 2012. Biosynthesis of silver nanoparticles using latex from few euphorbian plants and

their antimicrobial potential. Appl. Biochem. Biotechnol. 167, 776–790.
Perni, S., Hakala, V., Prokopovich, P., 2014. Biogenic synthesis of antimicrobial silver nanoparticles capped with L-cysteine. Colloids Surf., A 460, 219–224.
Prakash, P., Gnanaprakasama, P., Emmanuel, R., Arokiyaraj, S., Saravanan, M., 2013. Green synthesis of silver nanoparticles from leaf extract of *Mimusops elengi*, Linn. for enhanced antibacterial activity against multi drug resistant clinical isolates. Colloids Surf., B Biointerfaces 108, 255–259.
Prathna, T.C., Chandrasekaran, N., Raichur, A.M., Mukherjee, A., 2011. Biomimetic synthesis of silver nanoparticles by *Citrus limon* (lemon) aqueous extract and theoretical prediction of particle size. Colloids Surf., B Biointerfaces 82, 152–159.
Rastogi, L., Arunachalam, J., 2011. Sunlight based irradiation strategy for rapid green synthesis of highly stable silver nanoparticles using aqueous garlic (*Allium sativum*) extract and their antibacterial potential. Mater. Chem. Phys. 129, 558–563.
Romeo, J.T., 1984. Insecticidal imino acids in leaves of *Calliandra*. Biochem. Syst. Ecol. 12, 293–297.
Sathiya, C.K., Akilandeswari, S., 2014. Fabrication and characterization of silver nanoparticles using *Delonix elata* leaf broth. Spectrochim. Acta Part A Mol. Biomol. Spectrosc. 128, 337–341.
Shanmugam, N., Rajkamal, P., Cholan, S., Kannadasan, N., Sathishkumar, K., Viruthagiri, G., Sundaramanickam, A., 2014. Biosynthesis of silver nanoparticles from the marine seaweed *Sargassum wightii* and their antibacterial activity against some human pathogens. Appl. Nanosci. 4, 881–888.
Singh, K.P., Singh, A.K., Gupta, S., Rai, P., 2012. Modeling and optimization of reductive degradation of chloramphenicol in aqueous solution by zero-valent bimetallic nanoparticles. Environ. Sci. Pollut. Res. 19, 2063–2078.
Suman, T.Y., Rajasree, S.R.R., Kanchana, A., Elizabeth, S.B., 2013. Biosynthesis, characterization and cytotoxic effect of plant mediated silver nanoparticles using *Morinda citrifolia* root extract. Colloids Surf., B Biointerfaces 106, 74–78.
Tagad, C.K., Kim, H.U., Aiyer, R.C., More, P., Kim, T., Moh, S.H., Kulkarni, Sabharwal, S.G., . A sensitive hydrogen peroxide optical sensor based on polysaccharide stabilized silver nanoparticles. RSC Adv. 45, 22940–22943.
Tamboli, D.P., Lee, D.S., 2013. Mechanistic antimicrobial approach of extracellularly synthesised silver nanoparticles against gram positive and gram negative bacteria. J. Hazard. Mater. 260, 878–884.
Tamuly, C., Hazarikaa, M., Borah, S.Ch., Das, M.R., Boruah, M.P., 2013. In situ biosynthesis of Ag, Au and bimetallic nanoparticles using *Piper pedicellatum* C.DC: green chemistry approach. Colloids Surf., B Biointerfaces 102, 627–634.
Tavakoli, F., Salavati-Niasari, M., Mohandes, F., 2015. Green synthesis and characterization of graphene nanosheets. Mater. Res. Bull. 63, 51–57.
Theivasanthi, T., Alagar, M., 2012. Electrolytic synthesis and characterization of silver nanopowder. Nano Biomed. Eng. 4, 58–65.
Vijayakumar, M., Priya, K., Nancy, F.T., Noorlidah, A., Ahmed, A.B.A., 2013. Biosynthesis, characterisation and anti-bacterial effect of plant-mediated silver nanoparticles using *Artemisia nilagirica*. Ind. Crops Prod. 41, 235–240.
Wang, Q., Yun, Y., 2013. Nonenzymatic sensor for hydrogen peroxide based on the electrodeposition of silver nanoparticles on poly(ionic liquid)-stabilized graphene sheets. Microchima Acta 180, 261–268.
Wang, W., Chen, Q., Jiang, C., Yang, D., Liu, X., Xu, S., 2007. One-step synthesis of biocompatible gold nanoparticles using gallic acid in the presence of poly-(N-vinyl-2pyrrolidone). Colloids Surf., A 301, 73–79.
Wang, Y., Lu, J., Tong, Z., Huang, H., 2009. A fluorescence quenching method for determination of copper ions with CdTe quantum dots. J. Chil. Chem. Soc. 54, 274–277.
Yang, W., Yang, C., Sun, M., Yang, F., Ma, Y., Zhang, Z., Yang, X., 2009. Green synthesis of nanowire-like Pt nanostructures and their catalytic properties. Talanta 78, 557–564.
Zhang, W., Chen, Z., Liu, H., Zhang, L., Gao, P., Li, D., 2011. Biosynthesis and structural characteristics of selenium nanoparticles by *Pseudomonas alcaliphila*. Colloids Surf., B Biointerfaces 88, 196–201.